

## Characterization of collagen fiber loaded amino terminated hyperbranched polyamide and study on its adsorption property toward Cr(VI)

Wang xuechuan<sup>1,2\*</sup>, Zhang feifei<sup>1,2</sup>, Qiang taotao<sup>1,2</sup>, Wang xiaoqin<sup>1</sup>, Ren longfang<sup>1,2</sup>

<sup>1</sup>Shaanxi University of Science and Technology, Xi'an, Shaanxi, 710021, China, 8629-86132530

<sup>2</sup>Key Laboratory of Chemistry and Technology for Light Chemical Industry, Ministry of Education, Shaanxi University of Science and Technology, Xi'an, Shaanxi, 710021, China, 8629-86132662

\* [wxc-mail@163.com](mailto:wxc-mail@163.com)

### Abstract

In this study, we loaded amino terminated hyperbranched polyamide(HBPN) which is synthesized by methacrylate and diethylene triamine onto collagen fiber(CF) by glutaraldehyde to prepare novel adsorption material(CF-HBPN). X-ray photoelectron spectroscopy(XPS), thermal performance analysis and atomic force microscope(AFM) were employed to characterize the surface of CF and CF-HBPN. Furthermore, the adsorption performance toward Cr(VI) and thermodynamic property were studied. The experimental result indicated the Cr(VI) removal rate of CF-HBPN was 3.09 higher than that of CF under the same conditions. The removal rate increase with the increase of adsorption material dosage and decline with the increase of the initial concentration of the Cr(VI) solutions. When pH was about 3.0, the removal rate was the highest among other pH conditions. Langmuir isotherm adsorption models can describe the adsorption process better than Freundlich model. It's endothermic process, so the adsorption efficiency will be enhanced under a higher temperature. X-ray diffraction (XRD) was employed to elucidate the difference between CF-HBPN and CF-HBPN- Cr(VI).

**Keywords:** collagen fiber; amin terminated hyperbranched polyamide; glutaraldehyde; adsorption; Cr(VI)

### 1. Introduction

The biggest pollution of leather making industry was the chrome containing water generated by chrome tanning process. The concentration of chrome could reach to 3~8g/L in chrome tanning waste water (calculated by Cr<sub>2</sub>O<sub>3</sub>) (Altundogan 2005), which caused server environment pollution and resource waste. Cr(III) was essential micro mental element, but under some conditions, Cr(III) will be switched to Cr(VI). Cr(VI) has strong oxidative and migratory capability(Zhang et al. 2010). The toxicity of Cr(VI) was 100 times higher than Cr(III) (Rao et al. 2002). Cr(VI) contamination has arised great threaten to human health and environment.

Hyperbranched polymer is a kind of highly branching and it has three-dimensional

structure which endow it with unique cavity structure, massive functional groups, high activity and solubility, etc. The leather making process produce many discarded shavings. This kind of solid waste usually treated by landfill method which brought heavy pressure on environment and land use. Through acid expansion and physical treatment, the collagen fiber could be obtained by discarded shaving. Collagen fiber(Zhang et al. 2012) is a kind of environmental friendly natural macromolecule material which has amino and carboxyl groups. It can be used as the insoluble vector to prepare adsorbent. In this study, glutaraldehyde was used as cross-linking agent to load amino terminal hyperbranched polyamide onto collagen fiber. Large amount of nitrogen containing groups were induced onto collagen fiber to improve the adsorption property. A kind of novel adsorption material was prepared and applied in Cr(VI) containing waste water.

## 2. Material and methods

### 2.1 Experiment reagent and equipment

Hide and skin of pig, deionized water, potassium dichromate, diphenylcarbazide, methacrylate(MA), diethylene triamine(DETA) (AR, Tianjin Kemiou Chemical Reagent Co.), glutaraldehyde, AR, 50%, Tianjin Fuchen Chemical Reagent Co.; NaOH, HCl was analytically pure. PHS-3C precision acidimeter(Shanghai Leici Precision Instrument Factory), 722N visible spectrophotometer(shanghai precise scientific instrument Co.).

### 2.2 Synthesis of CF-HBPN

Collagen fiber(CF)(Cheng et al. 2007) and deionized water was added into 250mL three necked bottle, fully stirring to disperse, then add glutaraldehyde and amino terminated hyperbranched polyamide(Zhang et al. 2009) solution one by one by drops, under 40°C for 4h reaction, amino terminated hyperbranched polyamide collagen fiber (Wang et al. 2013) (CF-HBPN) could be obtained. Wash the CF-HBPN by deionized water fully to eliminate unreacted substance. Dry in 50°C vacuum drying chamber to constant weight. Milling the CF-HBPN and passing 100 size mesh to generate adsorbent. The synthesis route is shown in Fig.1.

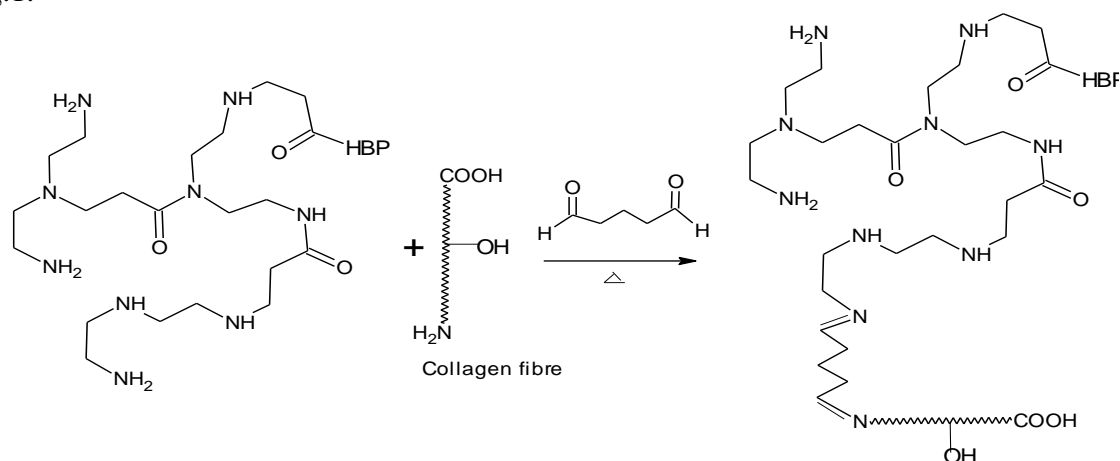


Fig.1 The synthesis route of CF-HBPN

### 2.3.2 Adsorption thermodynamics

Weight 0.4g CF-HBPN and add into triangular flask which contain 100mL different concentration Cr(VI) solution (pH was about 3.0), sealed the flask and then put them in constant temperature (293K, 303K, 313K) oscillator to react for 6h. Study on the influence of different reaction condition toward equilibrium concentration ( $C_e$ ) and equilibrium adsorption capacity ( $q_e$ ). Langmuir and Freundlich isothermal adsorption model (Danijela et al. 2012) were employed to fit the experimental data, then to elucidate the adsorption process.

Langmuir signal layer adsorption model suppose the surface of adsorption material (Nishtar et al. 2005) have certain amount of adsorption sites which are uniform distribution, the adsorption energy of adsorption site are same. The adsorption is signal layer. The simulation model equation is equation (3). Freundlich adsorption model suppose the adsorption material have different kind of adsorption sites (Wei et al. 2004). This model have wide range to use, it can be used in physical adsorption and chemical adsorption. The simulation model equation is equation (4).

$$C_e/q_e = 1/k_L + C_e/q_m$$

(3)

$$\ln q_e = 1/n \ln C_e + \ln k_F$$

(4)

In the equation,  $k_L$  is Langmuir adsorption constant,  $k_F$  is Freundlich adsorption constant,  $q_m$  is saturated adsorption capacity.

### 2.4 Characterization of modern analysis instrument

Take some CF and CF-HBPN sample to analysis by K-Alpha X-ray photoelectron spectroscopy. The sample was provoked by Al Ka ray (1486.6eV), the vacuum of analysis room is  $3 \times 10^{-7}$  torr. Use ultra low energy electric beam to neutralize the charge on sample's surface. The TG-DTG analysis is employed by the STA409PC thermal performance analysis to analysis. AFM analysis is occurred on SPI3800N/SPA400 atomic force microscope (Rigaku). The CF and CF-HBPN-Cr(VI) XRD analysis is happened on D/max2200PC X-ray diffraction (Rigaku). The pipe pressure is 60kV, the pipe flow is 80mA, the scanning speed is 0.1~24°/min.

## 3 Result and disccution

### 3.1 The XPS analysis of CF and CF-HBPN

#### (1) XPS wide scanning analysis

The wide scanning XPS spectrum of CF and CF-HBPN are in Fig.2, the relative data is shown in Tab.1. There are strong peaks in the binding energy of 285.08eV and 533.08eV, which indicated the main element consist is C, O and little N element (400.08eV). which indicated the surface of CF component changed after loaded HBPN.

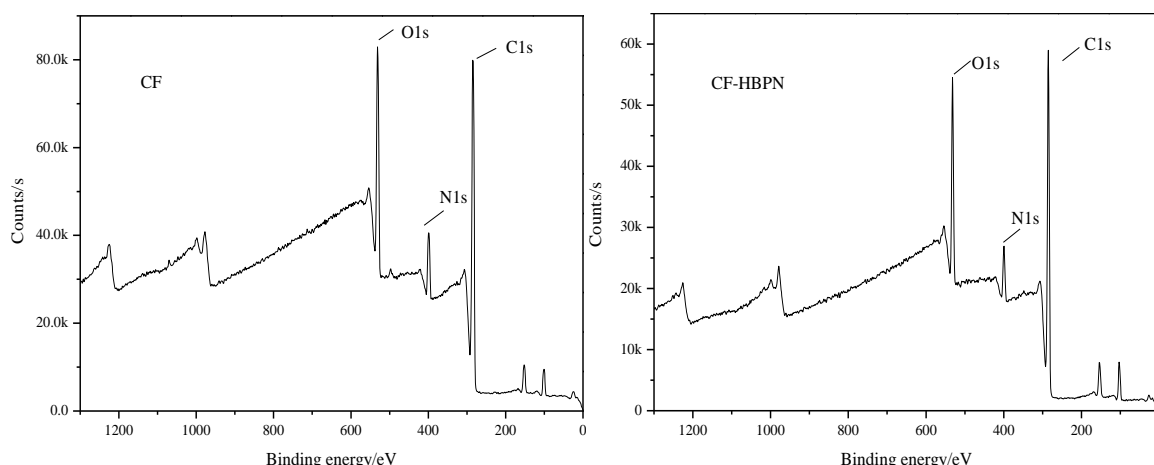


Fig. 2 XPS survey scanning spectra of CF and CF-HBPN

## (2) High resolution XPS analysis

The C<sub>1s</sub>, N<sub>1s</sub> and O<sub>1s</sub> high resolution XPS spectrum of CF and CF-HBPN are in Fig.3. The C<sub>1s</sub> spectrum of CF contains 4 peaks, the binding energy in 284.38eV is the carbon in -C-C-, -C-N and -C-H, the binding energy in 285.33eV is the carbon in -C-O and hydrogen bond (John et al. 2008; Murphy et al. 2009). The binding energy in 288.43 eV is the carbon in -NH-C=O, the binding energy in 291.43eV is the carbon in carboxylate radical (-O-C=O) (Annandurai et al. 2002). This mean the carbon in CF mainly consist by carbon connected with oxygen. After loaded HBPN, the C<sub>1s</sub> spectrum contain 4 peaks, the binding energy in 284.05eV is the carbon in -C-C-, -C-H- and -C-N-, the binding energy in 285.87eV is carbon in -C=N- and -NH-C=O, the binding energy in 287.98eV is the carbon in -N-C=O, the binding energy in 290.42eV is carbon in carboxylate radical. Compared the C<sub>1s</sub> spectrum of CF and CF-HBPN, the -C=N- specific peak appeared in the C<sub>1s</sub> spectrum of CF-HBPN which means the Schiff base formed by the glutaraldehyde when loaded HBPN onto CF. At the same time, the amount of carbon connected with oxygen and connected with carbon and hydrogen in CF-HBPN decreased, it is correspond to the formation of HBPN, in which the carbon is mainly connected to nitrogen and less connected to oxygen, so there might be many HBPN connected on the surface of CF.

There are 3 peaks in N<sub>1s</sub> spectrum of CF, the peak in 399.84eV is the nitrogen in -NH<sub>2</sub> (Pu et al. 2006), the peak in 401.32eV is the nitrogen in -NH-, the peak in 403.32eV is the nitrogen in -N-. The 3 peaks in N<sub>1s</sub> spectrum of CF-HBPN are as following: 398.48eV(-NH<sub>2</sub>), 400.22 eV(-NH-), 402.33 eV(-N-). Compared the N<sub>1s</sub> spectrum of CF and CF-HBPN, the nitrogen in -NH<sub>2</sub> of the surface of CF-HBPN decreased, the nitrogen in -NH- and -N-increased, this might because the glutaraldehyde react wit the -NH<sub>2</sub> on CF and CF-HBPN which result in the decreased of the amount of -NH<sub>2</sub>. so the HBPN is loaded on the surface of CF successfully. At the same time, this indicated that the increasing of CF-HBPN's adsorption property might on account of the increasing of the nitrogen contained groups amount on the surface of CF-HBPN as well as the three-dimensional structure and the cavity structure of HBPN.

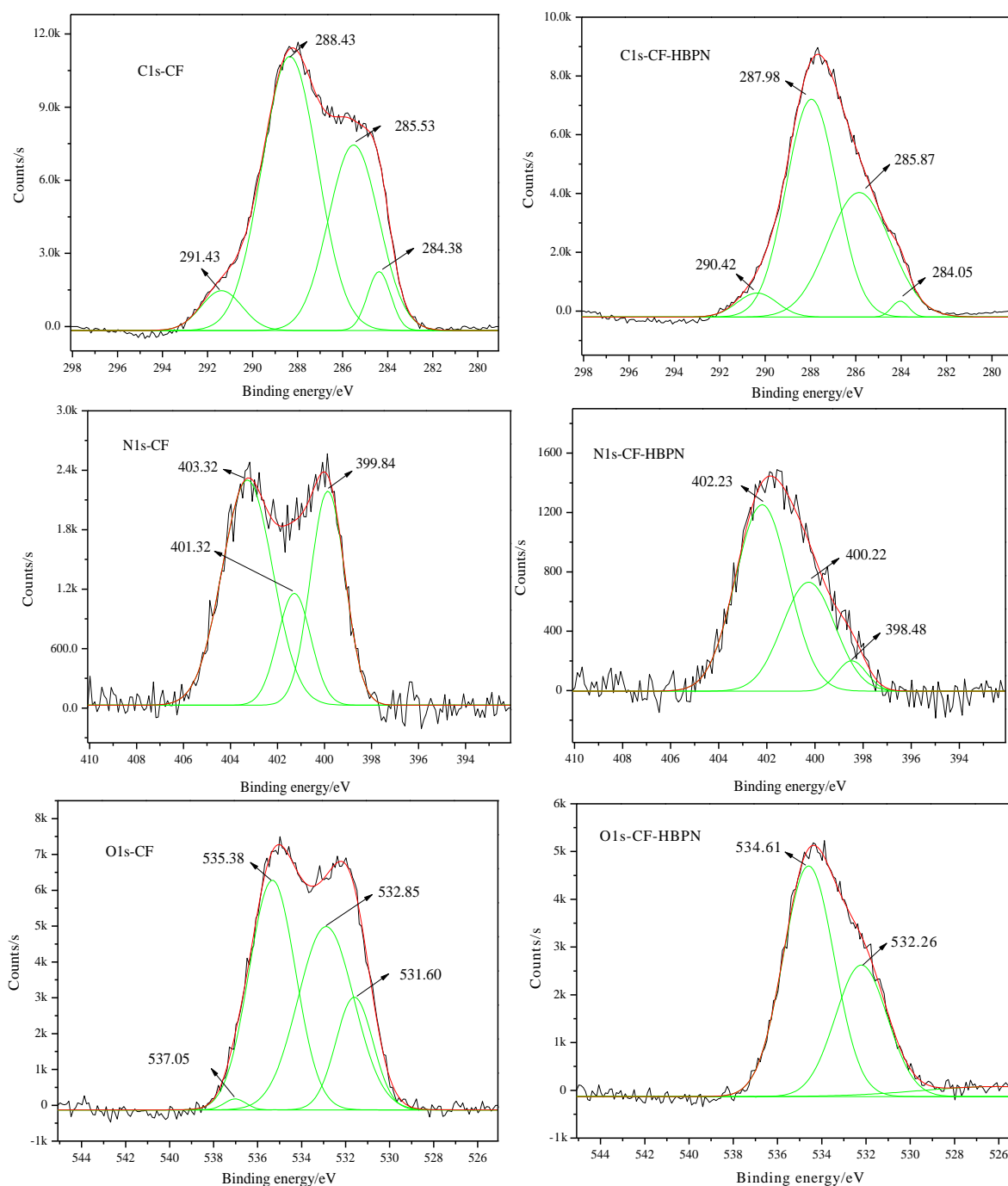


Fig. 3 High-resolution XPS spectra of CF and CF-HBPN

There are four peaks in O<sub>1s</sub> spectrum in CF, the peak in 531.60eV is oxygen in HO-C=O, the peak in 532.85eV is the oxygen in -N-C=O (Li et al. 2012), the peak in 535.38eV is oxygen in -C=O-O-R and -C=O, the peak in 537.05eV is the oxygen in -C-O-. But there are only 2 peak in CF-HBPN, they are the peak in 532.26eV of the oxygen in -C=O-O- and 534.61eV of oxygen in -N-C=O. This might because there are only two kinds of oxygen in different chemical environment, this is corresponding to the structure of HBPN. The XPS spectrum analysis indicated that the system react by the Fig.1.

### 3.1.2 The thermal property of CF and CF-HBPN

The combustion characteristic curves of CF and CF-HBPN are shown in Fig.5. The DTG curve of CF occur the double peaks which corresponding to the research results of Liang (Xu et al. 2007). While one peak applied in the DTG curve of CF-HBPN, this might because under the cross-linking function of glutaraldehyde, the structure of CF changed. When the temperature raised to 150°C, most moisture in CF and CF-HBPN separate out. The thermal property analysis indicated that when the temperature arised to 600°C, the total weight loss of CF is 73.26% while 67.77% of CF-HBPN. The kindng temperature of CF is 204.22°C while 265.12°C of CF-HBPN. The maximum weight loss rate temperature of CF is 310.9°C, The first peak is the burning stage of volatile component, the weight loss is 32.82%, the second peak is the fixed carbon burning stage, the weight loss is 40.44%. The burnout temperature of CF and CF-HBPN are 474.74°C and 534.01°C respectively. The specific temperature of CF and CF-HBPN above indicated the thermostability of CF increase after loaded HBPN by glutaraldehyde.

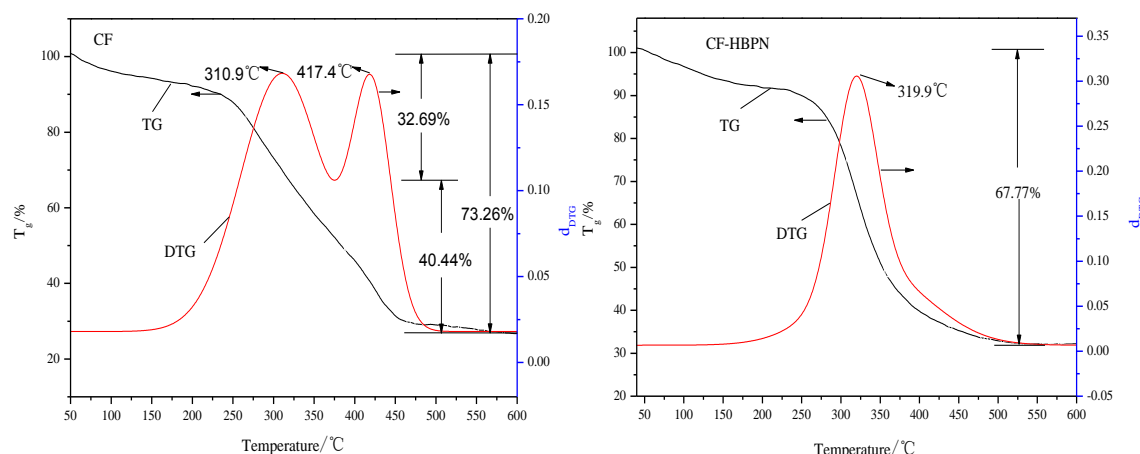


Fig.5 The TG-DTG curves of CF and CF-HBPN

### 3.1.3 The AFM characterization of CF and CF-HBPN

The section figures of CF and CF-HBPN are shown in Fig.6. Compared the A and B figure in Fig.6, the change of total height of the surface of CF isn't obvious while that of the CF-HBPN is obvious (Qu et al. 2005). The AFM morphology of CF-HBPN is corresponding to the research result of hyperbranched polyamide by Liu (Liu et al. 2007). This indicated the HBPN loaded on the surface of CF. The three-dimensional figures of the CF and CF-HBPN are shown in Fig.7. The surface morphology changed after modification. The comprehensive roughness of CF-HBPN (Fig.7 B) is higher than CF (Fig.7 A) which is benefit to enhance the adsorption property.

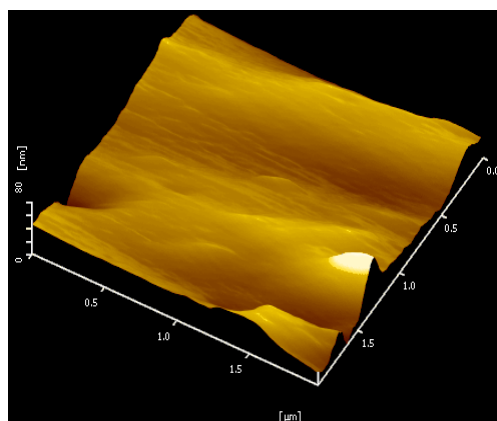
## 3.2 Adsorption property research and characterization

### 3.2.1 The comparison between CF and CF-HBPN

Add 4g/L CF and CF-HBPN into 100mL Cr(VI) containing solution whose initial

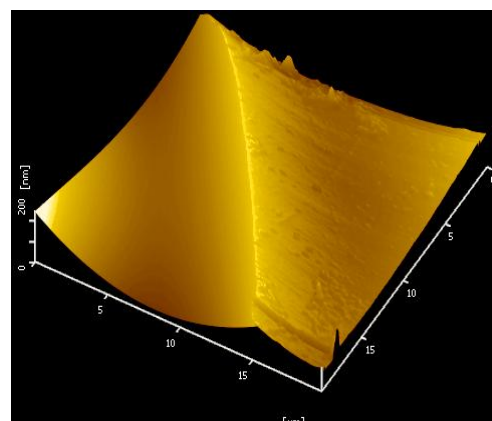


concentration is 50mg/L(pH is about 3.0 ). Put it into 30°C constant oscillator for 6h reaction. The experiment result shown in Fig.8. After 6h reaction, the removal rate of CF toward Cr(VI) is 24.53%, the adsorption tend to steady. At the same time, the removal rate of CF-HBPN toward Cr(VI) is about 94.31% after react for 5min. After react for 20min, the adsorption tend to steady, the removal rate is 99.57% when the adsorption reach to balance. Compared to CF, the removal rate of CF-HBPN is 3.09 times higher than CF, the previous targets are obtained.



Ra=9.563E+00nm

H=80nm



Ra=2.797E+01nm

H=200nm

Fig.7 The surface morphology images of CF and CF-HBPN

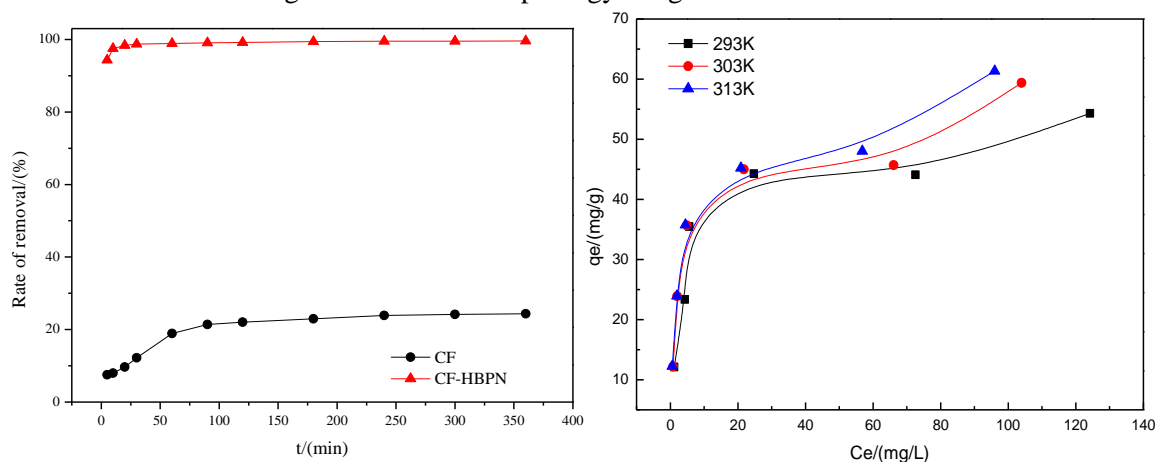


Fig.8 Comparison of CF and CF-HBPN on Cr (VI) removal Fig. 10 The adsorption isotherm of CF-HBPN toward Cr(VI)

### 3.3 Adsorption thermodynamics

#### 3.3.1 Adsorption isotherm

The fitting result of Langmuir and Freundlich adsorption model are shown in Fig.11. Compared the correlation coefficient ( $R^2$ ) of the fitting result, the langmuir adsorption model can describe the adsorption process of CF-HBPN toward Cr(VI). The adsorption isotherm parameter of the fitted result is shown in Tab.2. The fitted data about the saturated adsorption capacity(qm) are similar with the experimental result of equilibrium adsorption capacity (qe).

The physical adsorption is based on the van der Waals existed between the molecular which happened on the surface of adsorption material, the adsorption usually is the multi-layer adsorption. While the chemical adsorption usually is the signal layer adsorption, so the adsorption between CF-HBPN and Cr(VI) has physical adsorption and chemical adsorption, while chemical adsorption is dominated.

The difficult degree of the adsorption process could be measured by infinitude dispersion constant  $R_L$  [ $R_L=1/(1+bC_0)$ ] (Maksin et al. 2012), in the equation, the  $b$  is the langmuir adsorption constant]. When  $R_L=0$  or  $R_L>1$ , the adsorption is hard to occur, when  $R_L=1$ , the adsorption process occurred very easily, when  $0<R_L<1$ , the adsorption is easy to occur. When temperature is 303K, we calculated the  $R_L$ , the  $R_L$  of different initial concentration is in the range of 0.008~0.061, which indicated that the adsorption between CF-HBPN and Cr(VI) occur easily .

### 3.3.2 Thermodynamics parameter

The thermodynamics parameter Gibbs free energy change( $\Delta G$ , kJ/mol), adsorption enthalpy increment( $\Delta H$ , kJ/mol) and adsorption entropy( $\Delta S$ , kJ/(mol·K)) can be calculated by following equations. Cause the thermodynamics equilibrium constant  $k_a$  changed with temperature as the equation (5). The  $\Delta G$  can be calculated by Gibbs free energy equation (6), while the entropy can be calculated by Gibbs-Helmholtz equation (7).

$$\ln k_a = -\Delta H/RT + \Delta S/R \quad (5)$$

$$\Delta G = -RT \ln k_a \quad (6)$$

$$\Delta S = (\Delta H - \Delta G)/T \quad (7)$$

In the equation,  $R$  is the ideal gas constant, 8.314J/(mol·K);  $T$  is the absolute temperature, K;  $k_a$  is the thermodynamics equilibrium constant, L/g,  $k_a = bq_m$  (where  $b$  is langmuir adsorption constant).

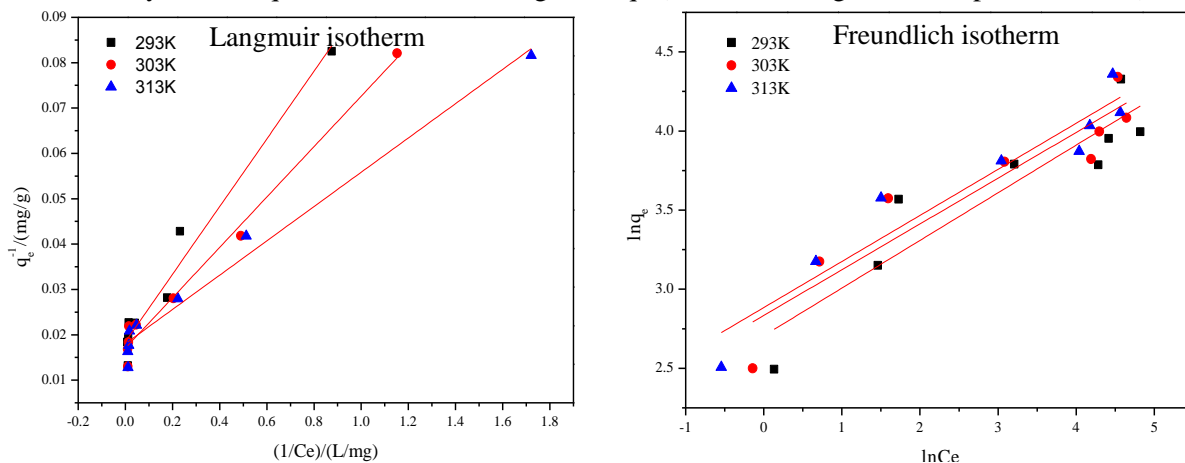


Fig. 11 Langmuir, Freundlich isotherm of CF-HBPN toward Cr(VI)



Tab. 2 Langmuir, Freundlich isotherm parameter of CF-HBPN toward Cr(VI)

| T/K  | Langmuir       |                |       | Freundlich     |                |       |
|------|----------------|----------------|-------|----------------|----------------|-------|
|      | R <sup>2</sup> | q <sub>m</sub> | b     | R <sup>2</sup> | k <sub>F</sub> | 1/n   |
| 293K | 0.963          | 54.259         | 0.247 | 0.831          | 14.966         | 0.301 |
| 303K | 0.983          | 58.617         | 0.307 | 0.857          | 17.011         | 0.289 |
| 313K | 0.977          | 60.463         | 0.477 | 0.903          | 17.880         | 0.291 |

Supposed the temperature doesn't influence the  $\Delta H$ ,  $1/T$  is treated as the horizontal coordinate while  $\ln k_a$  is vertical coordinate, then linear fitting, the equation of linear regression is obtained(8), the  $\Delta H$  can be calculated by the slope of regression equation.

$$\ln k_a = -3.5285(1/T) + 14.60423 \quad (R^2 = 0.9648) \quad (8)$$

The Thermodynamical parameters of the adsorption process is shown in Tab.3. The adsorption enthalpy increment  $\Delta H > 0$  which indicated the adsorption process is endothermic process, elevate the temperature is benefit the adsorption process.  $\Delta H > 24 \text{ kJ/mol}$ , which mean the adsorption of CF-HBPN toward Cr(VI) is not a simple physical adsorption but some ion exchange or chemical reaction occurred (Liu et al. 2011). The adsorption free energy  $\Delta G$  is negative, which meant the adsorption is spontaneous (Chen et al. 2011), with the increase of temperature, the degree of spontaneous is bigger. The adsorption entropy is always positive which meant the adsorption process is orderliness decreased, confusion degree increased.  $|T\Delta S| > |\Delta H|$ , which meant the adsorption process is dominated by entropy change, not the enthalpy change.

### 3.4 The XRD characterization of CF-HBPN and CF-HBPN-Cr(VI)

The CF-HBPN and Cr(VI) loaded sample [CF-HBPN-Cr(VI)] were characterized using XRD (X-ray diffraction) techniques. The results of XRD analysis (Fig. 12) demonstrate that identical peaks of the CF-HBPN-Cr(VI) match well with those of standard CF-HBPN and that no other crystalline after adsorption phases were present. However, it is clear that the intensity of all peaks in Fig. 12 decreased after Cr(VI) adsorption. This might because the regularity of the HBPN's polymer structure changed (Bi et al. 2012). The peak appeared around  $28.08^\circ$  appeared the Cr diffraction peak (Qiu et al. 2006). The peak shift from  $31.81^\circ$  to  $32.83^\circ$  indicates the oxidation of the surface of CF-HBPN following Cr adsorption (Saidur et al. 2012).

Tab. 3 Thermodynamical parameters

| T/K | $\Delta H/(\text{kJ/mol})$ | $\Delta G/(\text{kJ/mol})$ | $\Delta S/[\text{kJ}/(\text{mol} \cdot \text{K})]$ | $T\Delta S$ |
|-----|----------------------------|----------------------------|--|-------------|
| 293 | 29.3356                    | -6.3224                    | 0.12169  | 35.6552     |
| 303 | 29.3356                    | -7.2806                    | 0.12085  | 36.6176     |
| 313 | 29.3356                    | -8.7484                    | 0.12167  | 38.0827     |

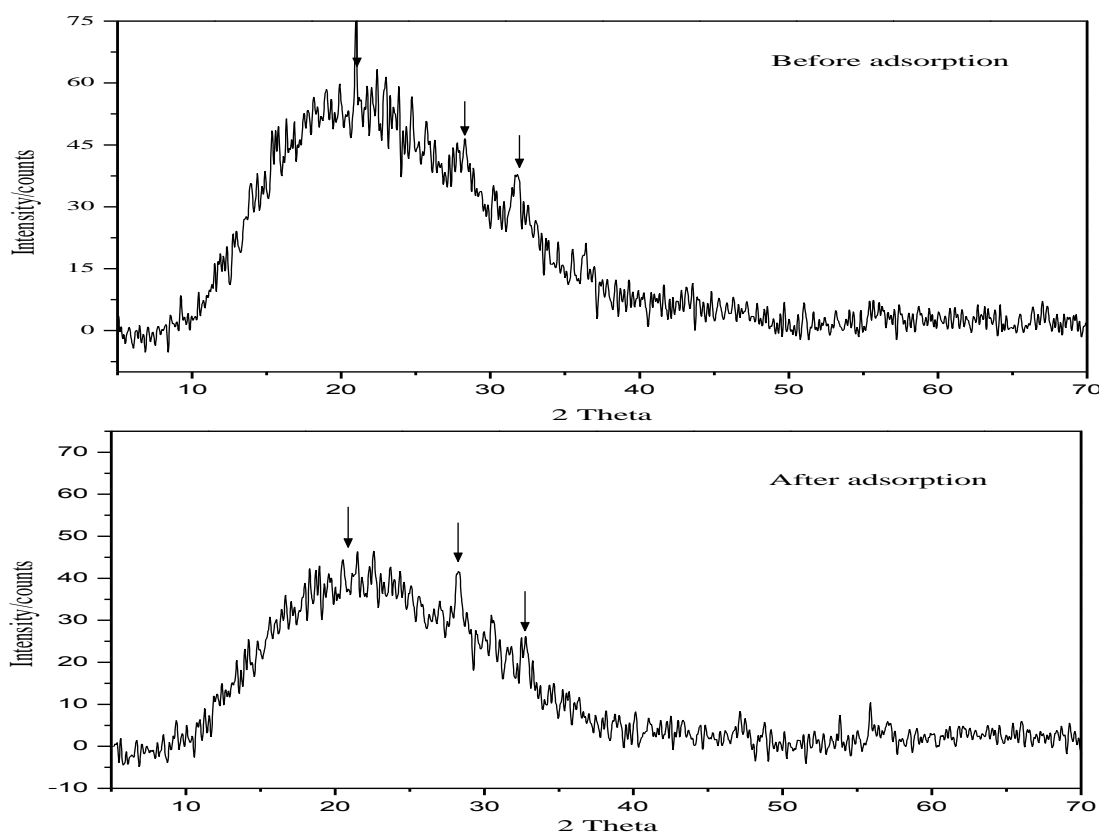


Fig. 12 The XRD spectrum of CF-HBPN before and after Cr(VI) adsorption

#### 4 Conclusion

Under the cross linking function of glutaraldehyde, we loaded HBPN onto CF to prepare novel adsorption material CF-HBPN. XPS, TG-DTG and AFM are employed to analysis the surface composition and thermal properties of CF and CF-HBPN. The experimental result indicated that the experiment react as the expect route. The adsorption prepare and thermodynamics was studied. Under the experimental condition, the removal rate of CF-HBPN is 3.09 times higher than CF, the maximum removal rate is obtained when pH is 3.0. The removal rate increase with the increase of dosage of adsorption material while decreased with the increase of initial Cr(VI) concentration. Langmuir adsorption isotherm model can describe the adsorption process better. The adsorption is endothermic process. XRD analysis result indicated that the surface of CF-HBPN occurred some oxidizing reaction after adsorb Cr(VI).

#### 5.Acknowledgements

This work was financially supported by the National Natural Science Fund (21076120), Science and Technology Project of of Shaanxi Provincial Government Education Department (12JK0594) and Science and Technology Project of Xianyang City (2011K10-11).

## 6.Reference

- [1] Altundogan H. S., 2005, Cr(VI) removal from aqueous solution by iron(III) hydroxide-loaded sugar beet pulp, *Process Biochemistry*, 40(3~4), 1443-1452p.
- [2] Zhang J. Y., Liang L. P., Pu L. J., Wang L. P., 2010, Adsorption Characteristics of Cr(VI) by Wheat Straw Including Kinetic and Thermodynamics Analysis, *Research of Environmental science*, 23(12), 1546-1552p.
- [3] Rao M., Parwate A.V., Bhole A.G., 2002, Removal of Cr(VI) and Ni(II) from aqueous solution using bagasse and fly ash, *Waste Manage*, 22(7), 821-830p.
- [4] Zhang Q. X., Zhang W. H., Liao X. P., Shi B., 2012, The study on separation and purification of apigenin using collagen fiber adsorbent, *Journal of functional material*, 5(43), 618-621p.
- [5] Cheng H. M., Wang R., Wang Y. M., 2007, Preparation and Characterization of Acid Relaxed Collagen Fiber from Pigskin, *Journal of Sichuan University(Engineering Science Edition)*, 39(3), 78-82p.
- [6] Zhang F., Chen Y. Y., Zhang D. S., 2009, Preparation and Properties of Amino-Terminated Hyperbranched Polymers and Its Quaternary Ammonium Salt, *Polymer Materials Science & Engineering*, 25(8), 141-144p.
- [7] Wang X. C., Zhang F. F., Qiang T. T., 2013, Characteristic and Adsorption Mechanism of Hyperbranched Collagen Fiber toward Cr(VI), *Journal of functional material*, 44(4), 1-5p.
- [8] Danijela D. Maksina, Aleksandra B. Nastasovic, Aleksandra D. Milutinovic-Nikolic, etc., 2012, Equilibrium and kinetics study on hexavalent chromium adsorption onto diethylene triamine grafted glycidyl methacrylate based copolymers, *J. Hazard. Mater.*, 12, 209-210, 99-110p.
- [9] Nishtar Nishad Fathima, Rathinam Aravindhana, Jonnal agadda Raghava Rao, 2005, Solid Waste Removes Toxic Liquid Waste: Adsorption of Chromium(VI) by Iron Complexed Protein Waste, *Environ. Sci. Technol.*, 39, 2804-2810p.
- [10] Wei R. X., Chen J. L., Chen L. L., 2004, Study of the Adsorption Thermodynamics and Kinetics of Lipoic Acid onto Three Types of Resin, *Adsorption Science & Technology*, 27(7), 523-534p.
- [11] John F. Watts, John Wolstenholme, 2008, An introduction to surface analysis by XPS and AES, East china university of science and technology.
- [12] Murphy, V., Tofail, S. A. M., Hughes, H., McLoughlin, P., 2009, A novel study of hexavalent chromium detoxification by selected seaweed species using SEM-EDX and XPS analysis, *Chem. Eng. J.*, 148, 425-433p.
- [13] Annandurai G., Juang R. S., Lee D. J., 2002, Use of cellulose-based wastes for adsorption of dyes from aqueous solutions, *J. Hazard. Mater.*, 92(3), 263-274p.
- [14] Pu M., Ji J., Li X. L., Shen J. C., 2006, Surface Tailoring of PET via Immobilization of Comb-shaped Poly(ethylene glycol) for Promoting Endothelial Cell Compatibility, *Chemical Journal*

of Chinese Universities, 27(5), 951-955p.

[15] Li K. B., Wang Q. Q., Dang Y., Wei H., Luo Q., Zhao F., 2012, Characteristic and Mechanism of Cr(VI) Biosorption by Buckwheat Hull from Aqueous Solutions, *Acta Chimica Sinica*, 70(7), 929-937p.

[16] Xu C. F., Sun X. X., 2007, Combustion characteristic of biomass by using TG-DTG-DSC thermoanalysis, *Journal of Huazhong University of Science and Technology(Nature Science Edition)*, 35(3), 126-128p.

[17] Qu J. E., 2005, Studies on the Interfacial Behavior and Inhibition Mechanism of Inhibitors by Electrochemical Methods and AFM, *Huazhong University of Science and Technology*.

[18] Liu C. H., 2007., Preparation, Supramolecular Encapsulation, and Self-assembly of Hyperbranched Polymers, *Shanghai Jiao Tong University*.

[19] Maksin, D. D.; Nastasovic, A. B.; Milutinovic-Nikolic, A. D.; Surucic, L. T.; Sandic, Z. P.; Hercigonja, R. V.; Onjia, A. E., 2012, Equilibrium and kinetics study on hexavalent chromium adsorption onto diethylene triamine grafted glycidyl methacrylate based copolymers, *J. Hazard. Mater.*, 209-210, 99-110p.

[20] Liu H. H., Zhang S. S., Zhang S. Q., Luo P., Qiu C., 2011, Adsorptive Properties of an Adsorbent to Reactive Brilliant Red X-3B Prepared from Sludge and Coal by Co-Pyrolysis, *Research of Environmental Sciences*, 24(6), 704-710p.

[21] Chen D. L., Bai L. J., Huang Z. W., Ma S. M., Yuan A. Q., 2011, Kinetics and Thermodynamics of Cs on Aluminum Dihydrogen Tripolyphosphate, *Environmental Science & Technology*, 34(3), 105-108, 148p.

[22] Bi S. D., An X. Y., Dang M. Y., Liu Q. Y., 2012, Adsorption thermodynamics and kinetics of Cd(II) ions by modification of chitosan with vanillin, *Journal of Functional Materials*, 43(8), 1001-1004p.

[23] Qiu K. D., Li W. B., 2006, Adsorption of Hexavalent Chromium Ions on Multi-wall Carbon Nanotubes in Aqueous Solution, *Acta Physico-Chimica Sinica*, 22(12), 1542-1546p.

[24] Saidur Rahman Chowdhury, Ernest K. Yanfulb, Allen R. Pratt. 2012, Chemical states in XPS and Raman analysis during removal of Cr(VI) from contaminated water by mixed maghemite–magnetite nanoparticles, *J. Hazard. Mater.*, 235~236, 246-256p.